CIVIL ENGINEERING JOURNAL

Article no. 28

THE CIVIL ENGINEERING JOURNAL 3-2025

STUDY ON THE COMBINED IMPACT ABOUT JOINT DIP ANGLE AND ROCK THICKNESS ON THE EXCAVATION STABILITIES OF TUNNELS WITH LARGE-SPAN BASED ON NUMERICAL EXPERIMENT

Wen Wang[1], Yiqiao Liu[2], Jikang Yang[1], Jichun Hu[1], Huijian Zhang[2] and Lichuan Wang[3]

1. *CCCC Third Highway Engineering Bureau, Anding Wai Street, Dongcheng District, Beijing, 100010, China*
2. *Southwest Jiaotong University, School of Civil Engineering, Key Laboratory of Transportation Tunnel Engineering, Ministry of Education, No. 111, North Section, Second Ring Road, Jinniu District, Chengdu, Sichuan Province, 610031, China*
3. *China Railway 18th Bureau Group Co., Ltd., Tianjin, 300222, China; huijianz@163.com*

Received: 13.12.2024
Received in revised form: 15.07.2025
Accepted: 01.09.2025

ABSTRACT

The stability of the surrounding rock is intricately linked to joint characteristics, particularly when a tunnel traverses layered, jointed rock masses. However, existing research has predominantly concentrated on tunnel stability within single-jointed rock formations, considering large-span tunnels situated under complex geological conditions. Therefore, drawing upon the Chongqing Guobo Station Tunnel Project as a case study, this paper employs a numerical experimental approach to conduct an in-depth exploration of the relationship between joint dip angles, the thickness of jointed rock layers, and the stability of the tunnel's surrounding rock. The research findings reveal that variations in both joint dip angle and the thickness of jointed layers exert a substantial influence on the stability of the surrounding rock. Under different conditions, the maximum increase in tunnel deformation approaches 400 mm. As the dip angle changes, the deformation of the surrounding rock initially decreases and then increases. The disparity between displacement perpendicular to the joint surface and displacement along the bedding plane initially narrows and subsequently widens, eventually becoming predominantly governed by displacement along the bedding direction. Moreover, the location of maximum displacement gradually shifts from the arch shoulder to the tunnel crown. For large joint dip angles, the surrounding rock primarily undergoes tensile yield failure along the direction of the joint surface and shear yield failure perpendicular to it. When the thickness of the joint layer increases, both the displacement of the surrounding rock and the distribution range of the plastic zone diminish, which enhances the overall integrity and bolsters the stability of the surrounding rock.

KEYWORDS

Tunnel with large span, Numerical test, Influence rule, Surrounding rock stability

INTRODUCTION

In the Chongqing-Guizhou region, the geological setting is exceedingly intricate, characterized by a diverse array of adverse geological conditions. Among these, the layered jointed rock mass stands as a quintessential example. Guaranteeing the stability of the surrounding rock is of paramount importance for the safety of tunnel construction activities [1-3]. Notably, the existence of joints exerts a profound impact on the stability of the surrounding rock [4]. Owing to the cutting action within the joints, construction operations in certain soft rock masses may trigger a series of disasters. These include substantial displacement of the surrounding rock, block-falls from the tunnel crown, and cracking of the preliminary lining [5, 6]. Consequently, it becomes imperative to conduct in-depth research on the stability of tunnel excavation in laminated jointed rock masses. Such research is essential to fully ensure not only the safety but also the efficiency of tunnel construction endeavors.

Several studies have primarily centered on the failure mechanisms inherent in jointed rock masses [7, 8], highlighting that the dip angle of rock strata exerts a substantial influence on the mechanical behavior and failure patterns of rock specimens. In addition, scholars have also conducted a certain degree of research on the stability challenges associated with tunnels constructed in jointed rock masses [9]. Luo et al [10] found that for the steep dip angle of the joint, the stability of surrounding rocks was mainly affected by the nature of the rock mass, while for a slow dip angle, the joints are the key factors leading to damage to the surrounding rock. Suo et al [11] pointed out that the surrounding rock was the most stable if the dip angle of joints was in the range 45° ~ 60°. Zhou et al [12] found that the maximum extrusion deformation of the excavation face of a nodular rock tunnel was distributed in an ‘M’ curve centered at 90°, and the deformation was largest when the inclination angle was 60° and 120°. If the inclination angle increases, the damage form of the palm face was circular, triangular, and inverted triangular in that order. Li et al [13] analyzed the impact of inclination angles as well as the spacings of surrounding rock joints on tunnel deformation, and concluded that the tunnel displacement with the change of inclination angle shows a decrease and then an increase, and the lining control effect is positively correlated with the inclination angle. Zheng et al [14] found that the size and distribution density of joint inclination are negatively correlated with tunnel stability, in which joint inclination is the most critical factor affecting the stability of the surrounding rock. Tang et al [15] investigated the impact of laminated rock body on the stabilities of surrounding rock, and found that the displacement of surrounding rocks caused by the joint surface was the greatest in the direction of vertical joint surface, and the failure zone of surrounding rocks was also largely distributed along the directions in vertical joint surface. An in-depth analysis was conducted on the influence of dip direction on the main deformation zones of layered rock masses [16]. The findings revealed that the main deformation zones were prone to developing in areas where the normal direction of the rock layers is oriented towards the interior of the tunnel. Wang et al [17] delved into the impact of columnar joints on the stability of surrounding rock. Their study demonstrated that, in terms of the self-bearing capacity of the rock mass under various dip angles, the order from the weakest to the strongest is 45°, 60°, 75°, 90°, 30°, 0°, and 15°. Jiang et al [18] explored the failure characteristics of jointed rock in deep-buried tunnels at different inclination angles. They discovered that when the inclination angle of the fracture surface is either less than 70° or greater than 77°, stress-controlled failure serves as the primary failure mode. Conversely, stress-structural control failure occurs under other circumstances. Jia et al [19] investigated the effects of different dip angles of layered joints and lateral pressure coefficients on the stability of tunnels within jointed rock masses. Numerical analyses carried out in their study indicated that both the joint dip angle and the lateral pressure coefficient exert significant influences on the failure modes and deformation characteristics of tunnels. Jayakumar et al [20] analyzed the failure characteristics of tunnels under different fault dip angles. Their research found that when the dip angle is 60°, the structural force generated in the tunnel lining is greater.

In conclusion, while research into the influence of joints on the stability of tunnel surrounding rocks has yielded some notable achievements, a significant portion of the existing findings primarily pertains to medium and large-span tunnels. In contrast, relevant research on super - large - span tunnels remains relatively scarce. On the flip side, current studies have predominantly concentrated

on a single type of jointed rock mass. Consequently, the applicability of these existing research results to large-span tunnels with a complex composition of jointed rock masses, as well as the impact of geologic compliant bias, remains uncertain. In light of these gaps, this paper undertakes a systematic investigation into the effects of varying joint inclinations and rock thickness on the excavation stability of large-span tunnels. The study is based on the Chongqing East Ring Road Guobo Center Station project. Such research is instrumental in ensuring the safety and stability of the construction process and serves as a valuable reference for similar projects in the future.

PROJECT OVERVIEW

The Guobo Center Station of Chongqing East Ring Railway has a total length of 284m, with a burial depth ranging from approximately 23m to 55m, and an excavation width and height of 24m and 22m, respectively. The tunnel section area is approximately 449.6m^2, which belongs to the super large-span tunnel. The location of Guobo Station was displayed in Figure 1.

The tunnel is covered with miscellaneous fill at the top and passes through a stratified, jointed rock body, which is mainly composed of sandstone and mudstone. The rock stratum occurrence is S-N/38~40ºNW, with rock dip angles varying between 38° and 40°. The surrounding rock is fragmented and exhibits poor stability, primarily rated as Grade V. The exposed surrounding rock at the excavation faces of the tunnel is displayed in Figure 2.

Fig. 1 – Location of the Guobo Station

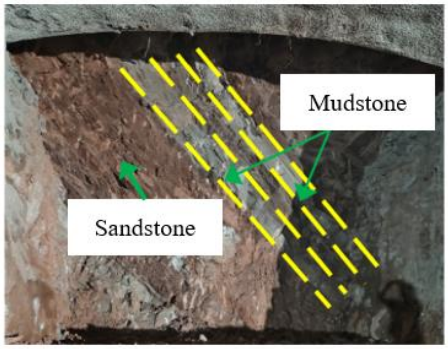

Fig. 2 – Joint Condition of rock mass in the on-site tunnel

NUMERICAL TEST MODEL AND CALCULATION INSTRUCTIONS

Drawing on the tunnel dimensions of the project under consideration, along with the stratigraphic distribution features and the objective of minimizing boundary-effect impacts, the ultimately adopted and established computational model is presented in Figure 3. The computational model has dimensions of length × width × height = 243 m × 60 m × 190 m. There is a

vertical distance of 110 m between the tunnel bottom and the base of the model. Normal constraints [21] have been applied to the front, back, left, right, and base surfaces surrounding the model. In contrast, the top surfaces are designated as free surfaces, allowing for unrestricted deformation. Regarding the initial stress conditions, only the gravitational stress field has been taken into account.

The mesh generation strategy has a huge impact on the calculation results. Therefore, a large number of mesh division trials were conducted before the start of this study. Considering the computational efficiency and accuracy, a local densification of the mesh was ultimately adopted in the area close to the tunnel, while a sparser mesh was used in the area far from the tunnel. Due to page limitations, the final adopted mesh division diagram is placed in this section, as shown in Figure 3.

The surrounding rock is simulated using solid zones, while joints were modeled with thinner solid zones and reduced mechanical parameters compared to the surrounding rock [22, 23]. Considering that the Mohr-Coulomb constitutive model can well characterize the shear failure of rock masses with high calculation efficiency, and the calculated parameters are convenient and accurate to obtain [24, 25]. Therefore, both the surrounding rock and the joints follow the Mohr-Coulomb ideal elastoplastic constitutive relation. Referring to the field geological survey of Guobo tunnel project and the data in *Code for Design of Railway Tunnels* [26], the computation parameter for the surrounding rock adopted in this paper is shown in Table 1.

Tab. 1 - Mechanically computation parameters of the surrounding rock

Surrounding rock	Elastic modulus *E* (MPa)	Poisson's ratio *μ*	Internal friction angle φ (°)	Cohesion c (kPa)	Density ρ (kg/m^3)
Miscellaneous fill soil	13	0.28	5	50	1800
Sandstone	1800	0.35	35	400	2200
Mudstone	130	0.38	24	65	2200

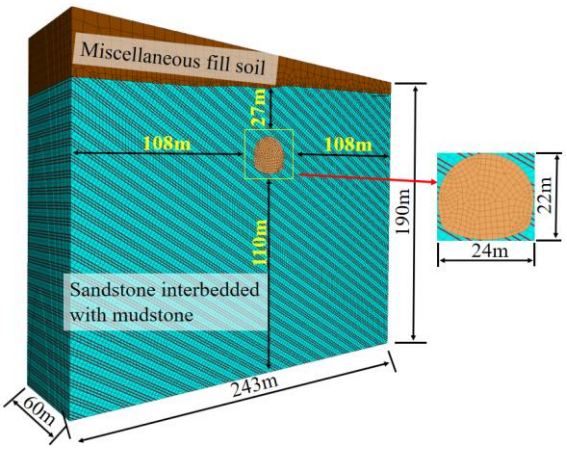

Fig. 3 – Calculation Model

To investigate the combined impact of jointed dip angles and variation in rock layer thickness on the stability of tunnels with large-span sections, the relevant calculated condition is displayed in Table 2.

Tab. 2 - Calculation condition

Variable name	Variable value			Remarks
Joint dip angle	30°	45°	55°	Fixed rock layer thicknesses of 1m
Rock layer thicknesses	1m	2m	3m	Fixed joint dip angle 45°

The tunnel is excavated by the full-face excavation method, with a cycle footage of 2 meters. No support is provided until the tunnel is excavated through. That is to say, the focus is on studying the impact of laws of jointed dip angles as well as rock layer thickness on the construction stability of super-large span tunnels without support, to offer a reference basis for the selection of tunnel lining methods in the subsequent dependent projects. The middle section (y = 30m) of the model is used as the monitored section, and the schematic diagram of the layout of monitored positions is displayed in Figure 4.

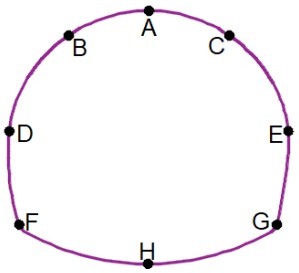

Fig. 4 – Layout of the monitoring point

ANALYSIS OF THE CALCULATION RESULTS

Discussion about tunnel stability under various joint dip angles

The cloud diagrams of surrounding rock displacement under various jointed dip angles are displayed in Figure 5. In Figure 5, the changes in jointed dip angles have very significant impacts on the displacement of the surrounding rock. For the jointed dip angle at 30°, the displacement of the surrounding rock in both the direction perpendicular to the jointed plane and the bedding direction is relatively large. Still, the displacement in the former direction is greater than that in the latter, and the maximum displacement is located near point B at the arch shoulder. For the jointed dip angle at 45°, the displacement of the surrounding rock in the bedding direction and the direction perpendicular to the joint plane are relatively close, and the maximum displacement appears between points A and B. For the jointed dip angle at 55°, the displacement of the surrounding rock in the bedding direction dominates, and the displacement perpendicular to the jointed plane is relatively small, with the maximum displacement appearing near point A. It indicates that during the addition of the jointed dip angle, the difference in displacement in the two directions first decreases and then increases. Eventually, the displacement in the bedding direction becomes dominant, and the location of maximum deformation of the surrounding rock moves from point B at the arch shoulder to point A at the crown, with the maximum displacement increasing from 43.2 mm to 437 mm.

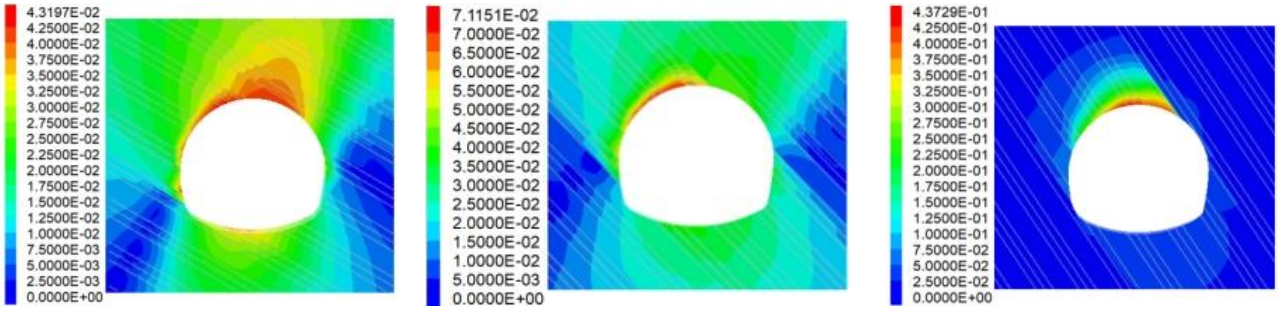

(a) 30° *(b) 45°* *(c) 55°*

Fig. 5 – Cloud diagrams of surrounding rock displacement under various jointed dip angles

The variation curves of surrounding rock displacement with the joint dip angles are displayed in Figure 6.

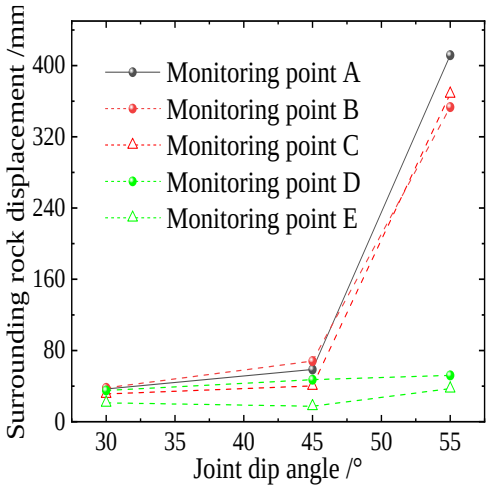

Fig. 6 – Diagram of the relationship between the displacement of tunnel surrounding rocks and jointed dip angles

In Figure 6, for the dip angle at 30° ~ 45°, although the surrounding rock displacement increases, the change is relatively slow. Nevertheless, when the dip angles varied within the range of 45° to 55°, notable increases in displacement are recorded at the vault and both arch shoulders. In comparison to the preceding angular variation range, monitoring points A, B, and C demonstrate growth rates of 600%, 360%, and 700%, respectively. As the dip angle changes, the characteristics of the stratum bias pressure also evolve, as evidenced by the fact that the displacement difference between the surrounding rocks on either side initially decreases and subsequently increases, reaching a maximum difference of 36 mm. Ultimately, the displacement observed at monitoring point C surpasses that at monitoring point B.

Figure 7 displays the cloud diagrams of the distributed state of the plastic area of the surrounding rock under various dip angles. Among them, the red part represents shear failure, and the black part represents tensile failure. The relationship diagram between the area ratio of the plastic zone of the surrounding rock to the tunnel sectional area (abbreviated as "R_{pt}") at various jointed dip angles is displayed in Figure 8.

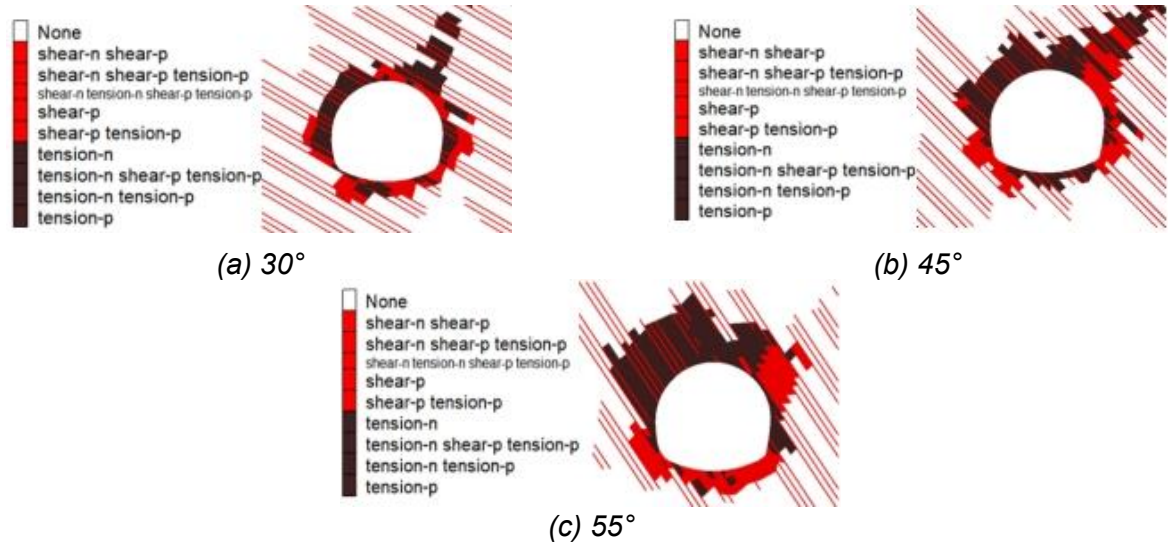

(a) 30° *(b) 45°*

(c) 55°

Fig. 7 – Cloud diagrams of the plastic zone of the surrounding rock under various joint dip angles

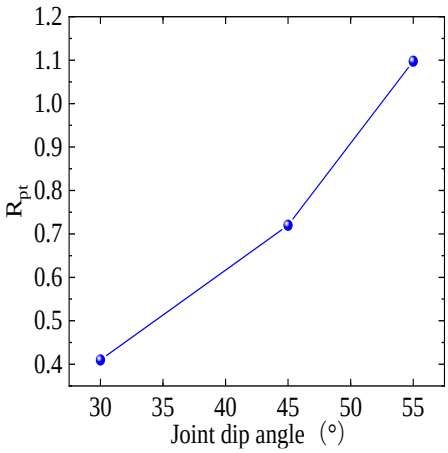

Fig. 8 – Diagram of the relationships between the R_{pt} and the jointed dip angles

In Figure 7, the weak interlayer is mainly subject to shear slip failure, and the distribution range of surrounding rock failure is mainly in the two directions perpendicular to the joints and along the joints. At little dip angles, shear failure predominates as the primary failure mode. If jointed dip angles increase, the distribution ranges of plastic zones in the two directions also change accordingly. The range along the joint plane direction gradually increases, while the range in the directions perpendicular to the joint plane slowly decreases. Finally, the failure mode along the joint plane direction is mainly tensile yield, and the failure in the directions perpendicular to the jointed plane is mainly shear yield. As the dip angle increases, the main failure mode of the rock mass changes from shear failure to shear-tension failure, which is consistent with the results of the model test [27]. Overall, the plastic area of the surrounding rock mostly appears above the center line of the tunnel, while yield zones on the left and right sides show an asymmetric distribution.

It can be seen from Figure 8 that R_{pt} also presents a nonlinear growth tendency with the increase of the dip angles, indicating that the jointed dip angle has a large influence on the failure of tunnel surrounding rocks, and the maximum increase rate of R_{pt} even reaches 0.7.

Discussion about the surrounding rock stability in a tunnel under different rock layer thicknesses

The cloud diagrams of the deformation of the tunnel surrounding rock under various rock layer thicknesses are displayed in Figure 9. The curve diagram of relationships between the displacement in the surrounding rock and variation of the rock layer thickness is shown in Figure 10.

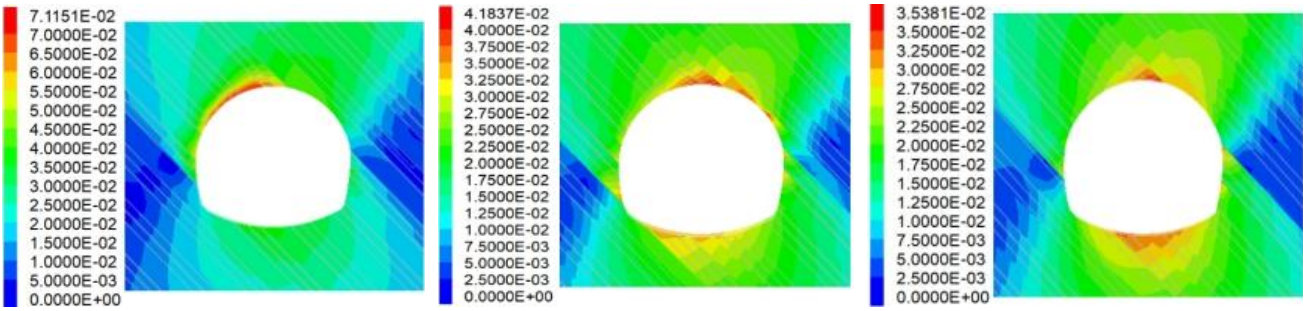

(a) 1m *(b) 2m* *(c) 3m*

Fig. 9 – The relationship between rock layer thickness and displacement diagram of the tunnel surrounding rocks

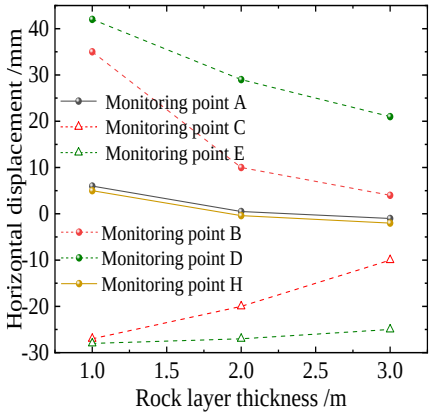

Fig. 10 – The relationships between the displacement of tunnel surrounding rocks and the variation of rock layer thickness

In Figures 9 and 10, for rock layer thickness at 1m, the displacement of the surrounding rock in the bedding direction and the direction perpendicular to the joint plane is relatively close. If the layer thicknesses increase, the deformation of the surrounding rock in the two directions basically remains consistent. This indicates that if joint dip angles remain constant, the changes in layer thickness hardly influence the difference in the distribution of surrounding rock deformation in different directions but have a relatively large impact on the magnitude of surrounding rock displacement. When the layer thickness increases, the displacement of the surrounding rocks at each monitoring position gradually decreases. Especially at the monitoring points B, C, and D, E, which are symmetrically distributed along the tunnel centerline, the variation in horizontal displacement of surrounding rocks gradually decreases; that is, the integrity of the rock mass becomes better. Since the increase in layer thickness brings about a reduction in the proportion of joints around the tunnel, thereby weakening the unbalanced pressure effect on the layer, as well as enhancing the stability of the surrounding rock. It is important to note that the horizontal displacement observed at vault point A and invert point H is nearly equal in magnitude and gradually converges towards 0 mm. This phenomenon can be attributed to the fact that these two points are vertical measurement locations, where horizontal displacement tends not to be significant.

The distribution of the plastic zone of the surrounding rock under various rock layer thicknesses is displayed in Figure 11. The variation of the R_{pt} of the tunnel with rock layer thicknesses is shown in Figure 12.

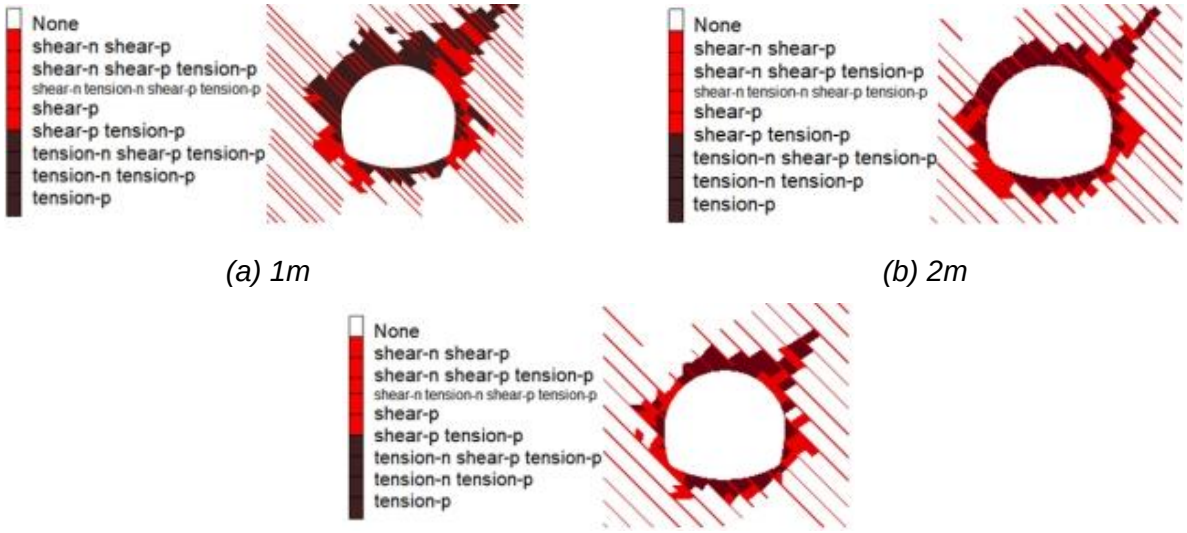

(a) 1m *(b) 2m*

(c) 3m

Fig. 11 – Diagram of relationships between the cloud diagram of the surrounding rock plastic area and the rock layer thickness

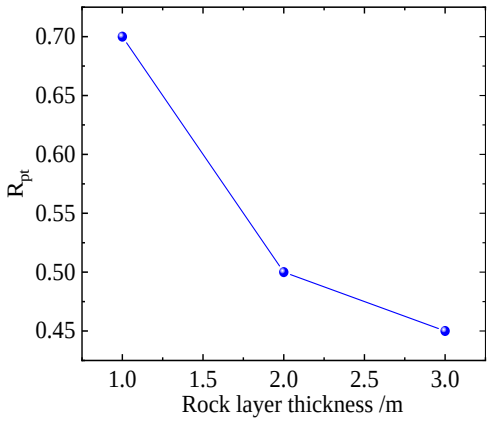

Fig. 12 – The relation curves between R_{pt} and rock layer thickness

It can be seen from Figures 11 and 12 that the failures range of the surrounding rock in the directions perpendicular to the joint and in the bedding direction are basically the same, and it is found that the thickness of the layer has a great influence on the distribution area of plastic area of the surrounding rock. When the layer thickness is 1m, the joints are distributed relatively densely, and the integrity of the rock mass is poor, resulting in a relatively large distribution area of the plastic zone, which is mainly distributed at arch waists. When the layer thicknesses increase, the spacing between joints gradually widens, the integrity of the rock masses improves, making them less susceptible to damage. Concurrently, the distribution area of plastic zones diminishes accordingly. As the layer thickness increases, the R_{pt} gradually decreases, the fragmentation degree of the surrounding rocks is reduced, and stability is enhanced. The maximum reduction rate of the R_{pt} reaches 0.25. Generally speaking, the thicknesses of the jointed layer have a direct effect on the stability of tunnel excavation. The smaller the joint spacing and the denser the distribution, the poorer the stability of the surrounding rock [14].

CONCLUSION

The main findings of this paper are listed below:

(1) The variation in dip angles exerts a profound impact on the displacement of the surrounding rock. When the dip angle is set at 30°, the displacement occurring in directions perpendicular to the joint plane surpasses that in the bedding direction. At a dip angle of 45°, the displacement of the surrounding rock in both the bedding direction and the direction perpendicular to the joint plane is relatively similar. Once the dip angle reaches 55°, the deformation of the surrounding rocks in the bedding direction becomes dominant. As the dip angles continue to increase, the growth rate of the surrounding rock's displacement initially exhibits a slow-paced trend, which then accelerates. The location of the maximum displacement gradually shifts from the arch shoulder towards the crown. Simultaneously, the difference in displacement between the two sides of the surrounding rock gradually widens, and the characteristics of unbalanced stratum pressure become increasingly prominent.

(2) Under varying joint dip angle scenarios, the plastic zone of the surrounding rock predominantly concentrates in two key directions: perpendicular to the joints and along the joints. Nevertheless, the extent of the plastic zone's distribution undergoes alterations in response to changes in the joint dip angle. As the dip angles gradually increase, the area encompassed by the plastic zone expands in a nonlinear fashion. In the case of large dip angles, the surrounding rocks are primarily subject to tensile yield failure along the direction parallel to the joint plane. Conversely, they mainly encounter shear yield failures in the direction perpendicular to the joint plane.

(3) When the dip angles are held constant, alterations in layer thickness exert minimal influence on the distribution pattern of surrounding rock deformation, whether in the direction perpendicular to the joint planes or along the jointed plane. However, they have a relatively significant impact on the magnitude of surrounding rock displacement. In scenarios where the layer thickness is small, the displacement of the surrounding rocks tends to be relatively substantial. As the layer thickness gradually increases, the displacement of the surrounding rock exhibits a corresponding decrease. Simultaneously, the disparity in displacement between the surrounding rocks on both sides of the tunnel diminishes. Consequently, the characteristics of unbalanced stratum pressure are mitigated, and the stability of the surrounding rocks is enhanced.

ACKNOWLEDGMENTS

This research was supported by the National Natural Science Foundation of China (Grant number: 52178395).

REFERENCES

[1] Kong W.Y., Zhou L.X., Wang J.L., 2024. Key technologies for quality control of tunnel lining construction of Xi'an-Kunming high speed railway. Railway Engineering, vol. 64, p. 96-100. http://doi.org/10.3969/j.issn.1003-1995.2024.07.17

[2] Yang Q.L., Li X., Wang Y.L., 2024. Discrete element numerical test of tunnel structure failure in fault fracture zones. Experimental Technology and Management, vol. 41, p. 136-142. http://doi.org/10.16791/j.cnki.sjg.2024.08.018

[3] Rong W., Su X.L., Zhao C.J., et al, 2024. Design of an experimental platform for investigating the structural response law of tunnel models crossing unfavorable geological zones. Experimental Technology and Management, vol. 41, p. 119-127. http://doi.org/10.16791/j.cnki.sjg.2024.07.016

[4] Lin C.B., Yu J., Chang F.Q., et al, 2023. Influence of three-dimensional persistent joints on surrounding rock stability of large-span tunnel. Journal of Central South University (Science and Technology), vol. 54, p. 1141-1152. http://doi.org/10.11817/j.issn.1672-7207.2023.03.030

[5] Liu X.Z., Liu W.Y., Suo C.F., 2014. Effects of the joint dip angle on the collapsed arch of surrounding rock around a highway tunnel. Modern Tunnelling Technology, vol. 51, p. 73-77. http://doi.org/10.13807/j.cnki.mtt.2014.06.012

[6] Pan W.T., He C., Wu F.Y., et al, 2023. Effect of bedding angle of layered soft rock tunnels with different large deformation grades. Journal of Civil and Environmental Engineering, vol. 45, p. 94-105. http://doi.org/10.11835/j.issn.2096-6717.2021.198

[7] Zhang Z.L., Wang, T., 2023. Failure modes of weak interlayers with different dip angles in red mudstone strata, Northwest China. Bulletin of Engineering Geology and the Environment, vol. 82, 156. https://doi.org/10.1007/s10064-023-03165-9

[8] Li Y.Z., Yuan L., Zhang Q.H., 2024. Brittle rock mass failure in deep tunnels: The role of infilled structural plane with varying dip angles. International Journal of Rock Mechanics and Mining Sciences, vol. 176, 105721. https://doi.org/10.1016/j.ijrmms.2024.105721

[9] Nikadat N., Marji M.F., 2016. Analysis of stress distribution around tunnels by hybridized FSM and DDM considering the influences of joints parameters. Geomechanics and Engineering, vol. 11, p. 269-288. https://doi.org/10.12989/gae.2016.11.2.269

[10] Luo S.L., Wu R.B., Zhang Z.Q., 2023. The influence of joint inclination angle and set number on stability of railway tunnel surrounding rock. Railway Investigation and Surveying, vol. 49, p. 48-53. http://doi.org/10.19630/j.cnki.tdkc.202302100001

[11] Suo C.F., Shi Y.D., Li J., 2013. Model test of effect of joint characteristics on stability of broken rock mass. Journal of Highway and Transportation Research and Development, vol. 30, p. 82-87. http://doi.org/10.3969/j.issn.1002-0268.2013.04.015

[12] Zhou J., Zhou Y., Chen L., et al, 2022. Influence of joint dip angle on deformation and instability mode of soft rock tunnel face. Subgrade Engineering, vol. 6, p. 196-200. http://doi.org/10.13379/j.issn.1003-8825.202205100

[13] Li J., Wu H.Q., Wang Y.J., et al, 2013. Analysis of the influence of joints characteristics and surrounding rock supporting on tunnel deformation. Construction Technology, vol. 42, p. 82-86. http://doi.org/10.7672/sgjs2013030082

[14] Zheng Y.C., Zhang W.S., Sun K.G., et al, 2020. Study on the stability of large-span tunnel by distinct element based strength reduction method. Modern Tunnelling Technology, vol. 57, p. 18-25. http://doi.org/10.13807/j.cnki.mtt.2020.01.00

[15] Tang R., An J.J., Xiang L., et al, 2019. Analysis of the impact of layered rock mass on stability of a highway tunnel. Modern Tunnelling Technology, vol. 56, p. 216-224. http://doi.org/10.13807/j.cnki.mtt.2019.S2.032

[16] Cui Z.D., Liu D.A., Wu, F.Q., et al, 2014. Influence of dip directions on the main deformation region of layered rock around tunnels. Bulletin of Engineering Geology and the Environment, vol. 73, p. 441-450. http://doi.org/10.1007/s10064-013-0511-6

[17] Wang L.X., Zhu Z.D., Zhu S., et al, 2023. A case study on tunnel excavation stability of columnar jointed rock masses with different dip angles in the Baihetan diversion tunnel. Symmetry, vol. 15, 1232. https://doi.org/10.3390/sym15061232

[18] Jiang, M.F., Feng, X.T., Zhao, J., et al, 2024. Time-dependent failure characteristics of natural jointed granite of deep tunnel under different dip angles conditions. Acta Geotechnica, vol. 19, p. 3075-3093. https://doi.org/10.1007/s11440-023-02201-y

[19] Jia P., Tang C.A., 2008. Numerical study on failure mechanism of tunnel in jointed rock mass. Tunnelling and Underground Space Technology, vol. 23, p. 500-507. https://doi.org/10.1016/j.tust.2013.07.017

[20] Jayakumar V., Visuvasam J.A., 2024. Numerical investigation on failure mechanism of tunnel lining with different fault dip angles and Geological Strength Index under geohazard of fault movement and seismic action. Geomatics Natural Hazards and Risk, vol. 15, 2363425. https://doi.org/10.1080/19475705.2024.2363425

[21] Xia Z.Y., Zhang C., Cao P., et al, 2023. Mechanical characteristics of large-section tunnel in soft rock based on various rock conditions and excavation footages. Stavební obzor-Civil Engineering Journal, vol. 32, p. 490-503. https://doi.org/10.14311/CEJ.2023.04.0037

[22] Zheng Y.R., Wang Y.F., Wang C., et al, 2011. Stability analysis and exploration of failure law of jointed rock tunnel-seminor on tunnel stability analysis. Chinese Journal of Underground Space and Engineering, vol. 7, p. 649-656. http://doi.org/10.3969/j.issn.1673-0836.2011.04.006

[23] Chen Q.C., Xu Q.F., Xie P.H., et al, 2023. Application of antisliding pile-key combination structure in gently inclined bedding rock slope with soft interlayer. Safety and Environmental Engineering, vol. 30, p. 131-140. http://doi.org/10.13578/j.cnki.issn.1671-1556.20221386

[24] Chai S.B., Hu J., Zhou Y.Q., et al, 2024. Influence of interface inclination angle of soft-hard strata on longitudinal mechanical properties of shield tunnel. China Railway Science, vol. 45, p. 135-146. http://doi.org/10.3969/j.issn.1001-4632.2024.05.13

[25] Pan H.W., Wu Y.C., Duan Y.X., et al, 2024. Optimization analysis of treatment scheme for metro tunnel base waterlogged collapsible loess formation. Urban Mass Transit, vol. 27, p. 261-265. http://doi.org/10.16037/j.1007-869x.2024.07.044

[26] National Railway Administration of the People's Republic of China, 2016. Code for Design of Railway Tunnels (TB 10003-2016). China Railway Publishing House, Beijing, p. 22.

[27] Song Z.P., Liu H.K., Zheng F., et al., 2023. Mechanical behavior and failure response characteristics of hard sandstones considering bedding dip angles. Coal Geology & Exploration, vol. 51, p. 167-175. http://doi.org/10.12363/issn.1001-1986.23.05.0227